

Leaf economic strategies drive global variation in phosphorus stimulation of terrestrial plant production

Received: 28 August 2024

Accepted: 30 May 2025

Published online: 01 July 2025

 Check for updates

Nan Yang^{1,2,3}, Constantin M. Zohner⁴, Thomas W. Crowther⁴, Jiguang Feng^{5,6}, Jin Wu^{7,8,9}, Xinli Chen¹⁰, Wenxuan Han¹¹, Benjamin D. Stocker¹², Dafeng Hui¹³, Laurent Augusto¹⁴, Kai Yue¹⁵, Enqing Hou^{16,17}, Mingkai Jiang¹⁸, Huili Feng¹⁹, Zixin Chen^{1,2,3}, Wenjuan Wu^{1,2,3}, Aijun Xing^{1,2,3}, Chengrong Chen^{20,21}, Jordi Sardans^{22,23}, Yiqi Luo²⁴, Josep Peñuelas^{22,23}, Hans Lambers²⁵, Jingyun Fang^{26,27} & Zhengbing Yan^{1,2,3} 

Plant biomass and its allocation are fundamental for understanding biospheric matter production. However, the impacts of atmospheric phosphorus (P) deposition on species-specific biomass and its allocation in global terrestrial plants remain unclear. By synthesizing 5548 observations of plant biomass and its allocation related to P addition worldwide, we find that P addition increases plant biomass by an average of 35% globally. This increase varies across plant functional groups, with stronger responses in deciduous (45%), C₃ (36%), and N₂-fixing plants (54%) than in evergreen (28%), C₄ (19%), and non-N₂-fixing plants (31%), respectively. Plants possessing traits indicative of an acquisitive strategy, such as higher nutrient concentrations and specific leaf area, faster photosynthetic rates and shorter leaf lifespan, are particularly responsive to P addition. Furthermore, P addition promotes a greater allocation of biomass to aboveground than belowground organs, resulting in a 5% decrease in root-to-shoot ratio. Our findings provide global-scale quantifications of how P addition regulates biomass accumulation and allocation strategies in terrestrial plants, offering critical insights for predicting the response of terrestrial carbon storage to rising atmospheric P deposition.

Plant biomass and its response to environmental changes significantly affect ecosystem function and global carbon cycles¹. Allocation of plant biomass among organs is crucial for growth, survival, and environmental acclimation², influencing carbon residence time in organs and carbon cycling within forest ecosystems³. However, nutrient availability, especially phosphorus (P), often constrains terrestrial plant biomass changes, as it is vital for growth, functioning, and reproduction⁴. In recent decades, anthropogenic P inputs from atmospheric deposition, livestock slurry manure applications, and mineral P fertilizers

have increased the P availability in terrestrial ecosystems^{5,6}. Such changes have substantial impacts on plant growth and biomass accumulation, thereby affecting ecosystem carbon stocks⁷. Despite this, prior studies mainly examined the effect of abiotic factors on aboveground biomass responses to P addition at the plant community level^{7,8}. Uncertainties persist about how biotic factors drive variation in plant biomass and allocation responses to P addition at the species level, posing challenges for accurate projection of future terrestrial carbon stock dynamics with continued global change.

One major source of uncertainties in plant responses to P lies in the diverse response patterns expected among different plant functional groups. This diverse response patterns fundamentally arise from the variation in P acquisition strategies, nutrient use strategies, and species-specific nutrient requirements⁹. For instance, shrubs with deep root systems and potent P-mobilizing exudates generally have a superior P acquisition ability from deeper soil layers and are better acclimated to low-P soils¹⁰. Conversely, graminoids with shallow root systems and fewer exudate releases may be more responsive to P addition¹¹. Nutrient use strategies, shaped by leaf habit and form, may also contribute to varying responses to P addition¹². Higher nutrient resorption efficiency can reduce dependence on soil nutrients and allow plants to conserve nutrients for survival in stressful habitats or to maintain high physiological activity during the growing season^{13,14}. Consequently, coniferous versus broadleaf species and deciduous versus evergreen plants—due to inherent differences in nutrient resorption efficiency¹⁴—are expected to exhibit distinct responses to P addition. Additionally, species differ in their intrinsic nutrient requirements. For instance, many N₂-fixing plants generally have a high P demand due to their limited ability to acquire P in low-P soils and the high energy cost of nitrogen (N) fixation¹⁵. Similarly, C₄ plants, which are inherently better adapted to P-poor habitats, tend to be less responsive to P addition than C₃ plants¹⁶. Consequently, plant responses to P addition are expected to vary considerably depending on growth form, leaf habit, leaf morphology, photosynthetic pathway, and N₂-fixing capability^{17,18}. However, variation in plants responsiveness to P addition among functional groups will be obscured at the plot level due to community interactions, which can mask species-specific patterns. Therefore, it is imperative to investigate plant responses to P addition at the species level.

In recent decades, the study of leaf functional traits has revealed key differences in resource use strategies among plant functional groups^{19,20}, which may impact plant responses to P addition. The leaf economics spectrum (LES) framework identified key functional traits that represent trade-offs between fast acquisition and conservation of resources²⁰. Specifically, species with an acquisitive strategy often exhibit greater specific leaf area (SLA), faster photosynthetic rates, higher leaf N and P concentrations ([N] and [P]), and shorter leaf lifespan. These traits contribute to rapid plant growth and biomass accumulation^{21,22}, potentially enhancing responsiveness to P addition. In contrast, species with a conservative strategy exhibit the opposite set of trait values, associated with slower growth and longer leaf lifespan^{22,23}, potentially making them less responsive to P addition. Therefore, trait variation across plant functional groups reflects distinct growth and resource use strategies, likely driving species-specific biomass responses to P addition^{24,25}. Accordingly, we hypothesize that leaf functional traits mediate plant biomass responses to P addition, with the magnitude of response increasing along the continuum from conservative to acquisitive LES strategies. However, empirical evidence supporting this hypothesis at a global scale is currently lacking.

Modifying biomass allocation among different plant organs is an adaptive strategy that maximizes resource utilization to support optimal plant growth and survival. This process is influenced by resource supply²⁶. The responses of the leaf, stem, and root mass fractions to resources supply are considered to be a functional equilibrium, such as the balance between photosynthetic carbon gain in leaves and nutrient uptake by the root system^{27,28}. When nutrient supply alters the resource balance, plants adjust their biomass allocation to restore an equilibrium adapted to the new conditions²⁹. For example, N addition typically leads to greater biomass investment in aboveground organs, increasing light interception and photosynthesis^{30,31}. According to the optimal partitioning theory, plant growth is maximized when biomass is proportionally allocated to the organs responsible for acquiring the most limiting resource³². Based on this framework, we hypothesize that P addition will similarly alter

resource availability, prompting plants to allocate more biomass to aboveground organs. However, globally, our knowledge regarding P-addition effect on biomass allocation patterns remains limited.

Here, we compile a global database from 317 publications, encompassing 5548 observations of plant responses to P addition across various controlled and field environments (Fig. 1a, and Supplementary Fig. 1 and Supplementary Tables 1 and 2), to quantify the effects of P addition on plant biomass and its allocation globally. We first estimate the average effect size across all terrestrial plant biomass responses and assess whether the effect size is influenced by evolutionary history. We also evaluate whether plant functional groups exhibit distinct responses to P addition by comparing the average effect size within each functional group. Second, we investigate the links between plant biomass response and leaf economics strategies as described by the leaf economics spectrum (LES). We further identify the key drivers of plant responses, including leaf functional traits, climatic factors, soil properties and fertilization regimes. Third, we quantify the effect of P addition on biomass allocation by estimating the average effect size for different plant organs and their respective mass fractions.

Results

Effects of P addition on plant biomass among plant functional groups

Across all terrestrial plants examined in this study, we observed that P addition led to a 35% increase (95% CI: 29.6–40.7%) in terrestrial plant biomass on average, with positive responses in 89% of all cases (Fig. 1c). We further examined the phylogenetic distribution of the P-addition effect on plant biomass and found no significant phylogenetic signal, as the effect sizes were similar among phylogenetic groups (Fig. 1b and Supplementary Fig. 2, $p > 0.05$). We then quantified the variation in the P-addition effect on plant biomass across various plant functional groups. Although there was no significant difference in the P-addition effect among growth forms ($p = 0.082$), we observed increases in biomass for tree (38%), shrubs (31%), graminoids (27%) and forbs (36%) (Fig. 2a). However, the P-addition effect did vary based on N₂-fixing taxa, leaf habit and photosynthetic pathway (Fig. 3a and Supplementary Fig. 3). Biomass significantly increased for N₂-fixing (54%, 41.2–67.2%) and deciduous plants (45%, 30.8–60.2%) when compared to non-N₂-fixing (31%, 24.7–36.8%) and evergreen plants (27.5%, 16.7–39.4%) (Fig. 3a and Supplementary Fig. 3, $p < 0.001$). Moreover, the P-driven biomass increase was greater in C₃ plants (36%, 30.2–42.2%) compared to C₄ plants (19%, 8.4–30.9%) (Fig. 3a and Supplementary Fig. 3). Lastly, the P-addition effect on plant biomass varied depending on the experimental setting, with generally greater effects observed in controlled environments compared to in field environments (Figs. 2b, 3b).

The links between plant biomass response and leaf economics traits

We further delved into the correlations of the P-addition effect on plant biomass with leaf functional traits and abiotic factors (i.e. climate variables, soil properties and fertilization regimes). These investigations revealed a dependence of the P-addition effect on leaf functional traits (Figs. 4 and 5). Specifically, the P-addition effect was significantly positively correlated with the first principal component (PC1) derived from a principal component analysis of multiple leaf functional traits (Fig. 4). This PC1 represents traits associated with an acquisitive strategy, such as thin leaves, high nutrient concentrations, fast photosynthetic rates, and short leaf lifespan. Furthermore, we observed significant positive correlations between the P-addition effect and both leaf [N] and SLA (Fig. 5 and Supplementary Table 3), and a significant, negative correlation with the leaf C:N ratio. Notably, these correlations were consistent across both controlled and field experimental settings (Fig. 5), highlighting the robustness of the correlations

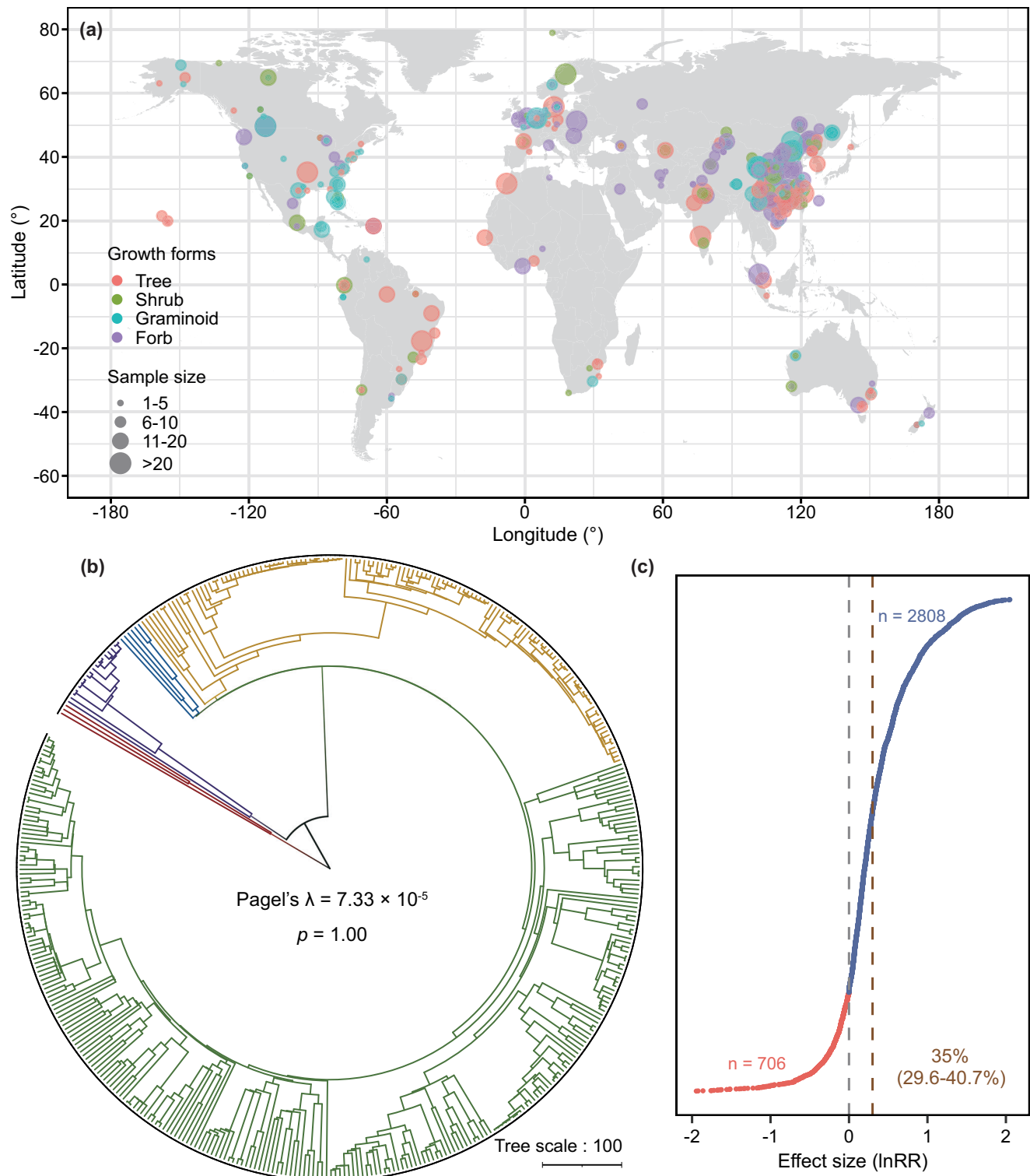


Fig. 1 | Geographical location, phylogenetic tree, and over effect sizes of phosphorus (%) addition on plant biomass. a Geographical location of study sites included in this meta-analysis. Different colored points represent different growth forms, with the point size indicating the number of observations for each site. The map was created using public-domain data from Natural Earth, accessed via the 'maps' package in R. **b** Phylogenetic tree of the 423 plant species assessed this meta-analysis. The phylogenetic signal in the effect sizes was estimated using Pagel's λ via maximum likelihood. A value of Pagel's $\lambda \approx 0$ and $p > 0.05$ based on a two-sided likelihood ratio test indicates an insignificant phylogenetic signal.

Different colored trees represent different phylogenetic groups. **c** The distribution of effect sizes of P addition on plant biomass. The lnRR indicates the log response ratio, and is quantified as the log-transformed ratio of plant biomass in P addition to the corresponding mean value of the control treatment; n represents the sample size for positive and negative effects of P addition on plant biomass. Dark blue and salmon indicate positive and negative effect sizes, respectively. Claybank dashed line represents the overall effect size as 35% (with 95% confidence interval in parentheses). Source data are provided as a Source Data file.

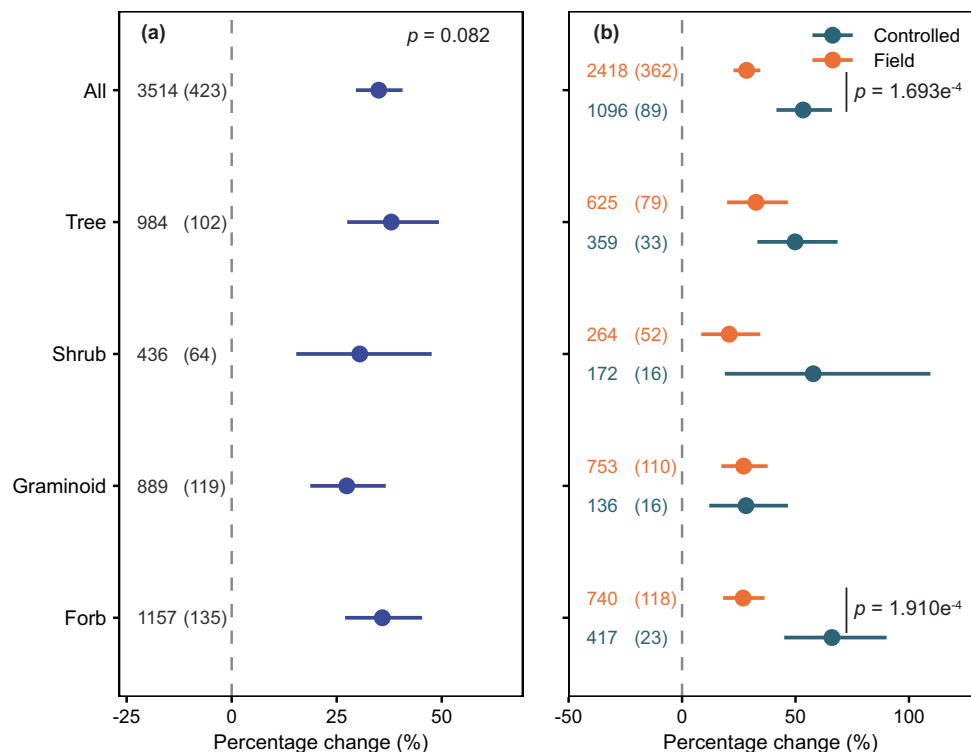


Fig. 2 | Effects of phosphorus (P) addition on plant biomass across growth forms and experimental settings. a Average effects (%) of P addition on plant biomass among growth forms for all data. **b** Average effects (%) of P addition on plant biomass under different experimental settings. Points and error bars represent the bootstrapped mean and 95% confidence interval, respectively. The numbers outside and inside parentheses indicate the number of observations and plant species, respectively. If the 95% confidence interval do not overlap zero, the effects

of P addition on plant biomass are considered significant (two-sided test, $p < 0.05$); otherwise, the effect of P addition is considered not significant. The p values indicate a significant level between growth forms or experimental settings, based on linear mixed models with 'growth form' or 'experiment type' as fixed factors and 'study' as a random factor, tested using two-sided F-tests with Satterthwaite approximation of degrees of freedom. Source data are provided as a Source Data file.

between these leaf traits and biomass response to P addition. These findings together suggest that plants with an acquisitive strategy are more responsive to P addition. Additionally, the P-addition effect was positively correlated with abiotic factors, such as mean annual temperature (MAT), mean annual precipitation (MAP), fertilization duration and P addition rates (Supplementary Fig. 4, and Supplementary Table 4). Conversely, negative correlations were found with soil total N and P concentrations and soil pH (Supplementary Fig. 5 and Supplementary Table 4), indicating that biomass responses to P addition are reduced in nutrient-rich soils.

To disentangle the influences of leaf functional traits from those of abiotic factors on P-addition effect on plant biomass, we first assessed the relative importance of these predictors using boosted regression tree (BRT) analyses. Results showed that both PC1 and key leaf functional traits (i.e. SLA, leaf [N], and leaf C:N ratio) that contributed to PC1 were the important driver of variation in the P-addition effect on plant biomass (Supplementary Figs. 6a, 7a). Partial dependence plots from the BRT models (Supplementary Figs. 6b, 7d, f, g) confirmed that the correlations of P-addition effect with PC1 and the key leaf functional traits derived were also consistent with those without controlling for other potential influencing factors (Figs. 4, 5). Furthermore, we evaluated the direct and indirect effects of leaf functional traits (indicated by PC1) and abiotic factors on plant biomass response (lnRR) through a structural equation modeling (SEM) analysis. The SEM results indicated that climate variables and soil properties had large indirect effects on lnRR through PC1, together with the largest direct effect of PC1 itself on lnRR (Fig. 6). Collectively, both BRT and SEM analyses robustly demonstrated that

leaf economic strategies importantly determined the variation in P-addition effect on plant biomass.

Effects of P addition on allocation of plant biomass

In addition to assessing plant biomass responses, we evaluated the effect of P addition on biomass allocation. Our results revealed that P addition had varying effects on the plant biomass of across organ types (Fig. 7a, $p < 0.001$). Leaf and stem biomass showed the strongest responses, increasing by 58% and 55%, respectively, followed by shoot biomass, which increased by 48%. In contrast, root and reproductive biomass showed significantly smaller responses to P addition, increasing by 40% and 35%, respectively ($p < 0.05$). Consequently, P addition shifted biomass allocation patterns, increasing leaf, stem and shoot mass fractions by 6% (1.1%–11.3%), 3% (–0.7%–7.1%), and 3% (0.5%–4.9%), respectively, while decreasing the root mass fractions and root-to-shoot ratios by 3% (–6.7%–0.6%) and 5% (–10.0%––0.6%), respectively (Fig. 7b). These findings suggest that P addition shifts the functional equilibrium between aboveground and belowground organs, promoting greater biomass allocation to aboveground organs. To further explore these dynamics, we investigated how P addition influences biomass allocation across plant functional groups, and its correlations with leaf functional traits and abiotic factors. Surprisingly, plant biomass allocation responses to P addition did not significantly differ among plant functional groups (Supplementary Fig. 8), and showed no significant correlations with either the PC1 depicting leaf economic strategies or individual leaf trait (Supplementary Figs. 9a–c, 10a). Abiotic factors also exerted very limited explanatory power on the response of plant biomass allocation (Supplementary Figs. 9d–f, 10a).

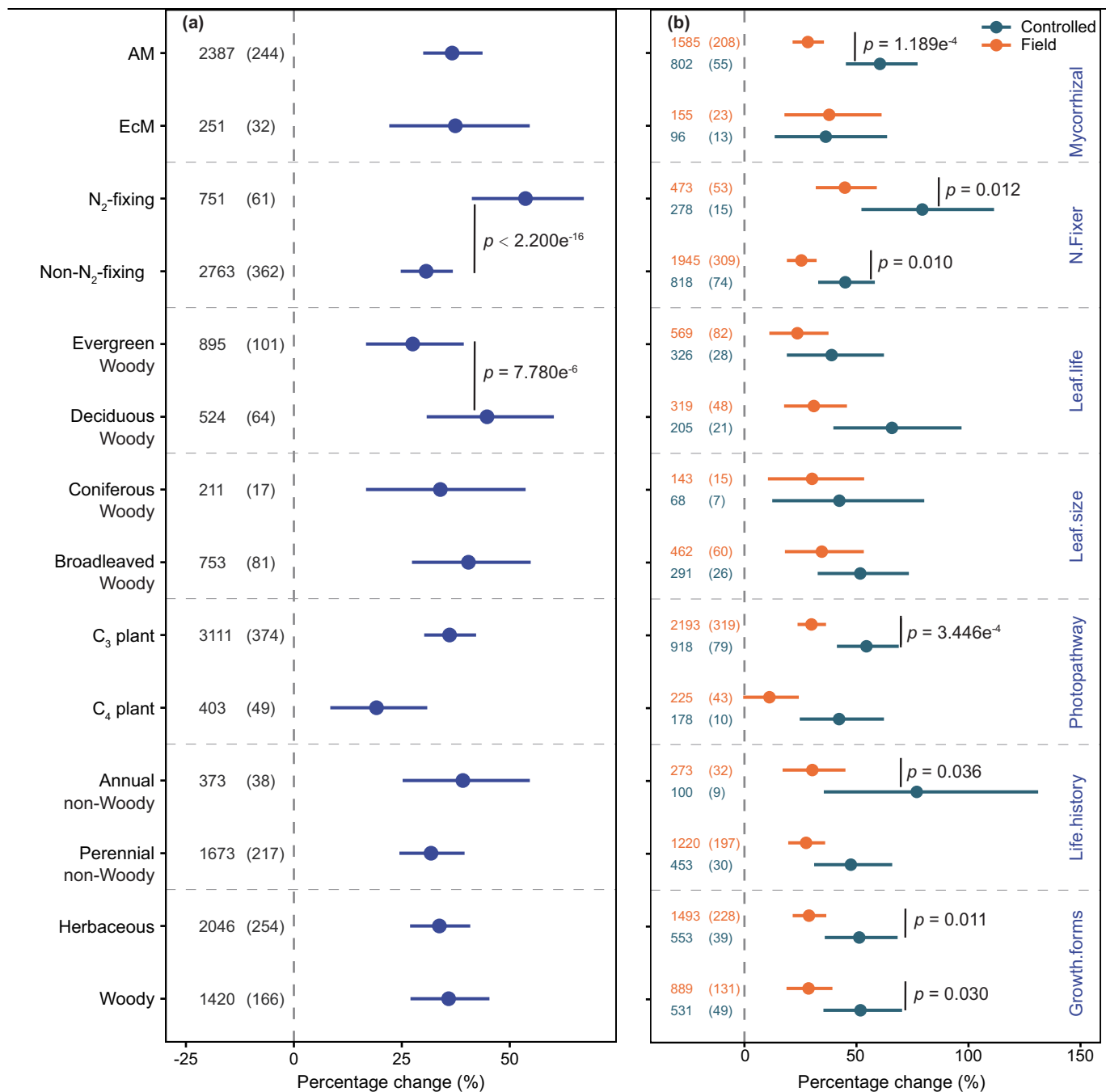


Fig. 3 | Effects of phosphorus (P) addition on plant biomass across plant functional groups and experimental settings. a Average effects (%) of P addition on plant biomass among plant functional groups for all data. **b** Average effects (%) of P addition on plant biomass under different experimental settings. Points and error bars represent the bootstrapped mean and 95% confidence interval, respectively. The numbers outside and inside parentheses indicate the number of observations and plant species, respectively. If the 95% confidence interval does not

overlap zero, the effects of P addition on plant biomass are considered significant (two-sided test, $p < 0.05$); otherwise, the effect of P addition is considered not significant. P values indicate significant level between experimental settings or functional groups, based on linear mixed models with 'experiment type' or 'functional type' as fixed factors and 'study' as a random factor, tested using two-sided F-tests with Satterthwaite approximation of degrees of freedom. AM arbuscular mycorrhizal, EcM ectomycorrhizal. Source data are provided as a Source Data file.

Discussion

Our meta-analysis provides a comprehensive overview of the effects of P addition on plant biomass and its allocation, identifying key drivers of variation in plant responses across the globe. We discovered that P addition, on average, augmented plant biomass by 35%, with the response to P addition being phylogenetically conserved (Fig. 1b, c). However, the degree of responsiveness varied based on plant N₂-fixing taxa, leaf habit, and photosynthetic pathway (Fig. 3). Biomass responses to P addition were strongly linked to leaf functional traits, with plants exhibiting acquisitive traits being more

responsive to P addition (Figs. 4–6). Moreover, P addition shifted biomass allocation patterns by increasing the mass fractions of leaves, stems and shoots (Fig. 7), suggesting a preferential allocation of biomass to aboveground organs in response to enhanced nutrient availability.

Plant functional groups, defined by N₂-fixing taxa, leaf habit, and photosynthetic pathway, influenced the response of plant biomass to P addition (Fig. 3a). N₂-fixing plants exhibited greater biomass accumulation under P addition than non-N₂-fixing plants (Fig. 3a). This enhanced response is likely due to the greater P demands of many N₂-

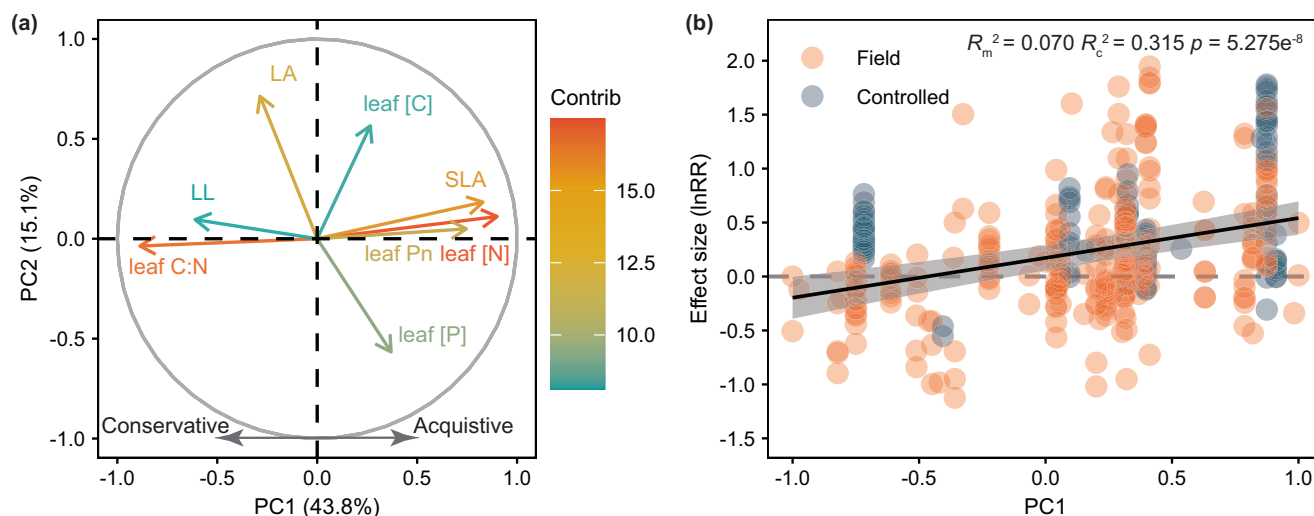


Fig. 4 | Correlations between the responses of plant biomass and leaf economics spectrum. **a** Principal component analysis (PCA) of leaf functional traits. The trait loadings are delineated by principal component 1 (PC1) and principal component 2 (PC2), with the color gradient of the arrows indicating their contribution to the principal components. **b** The correlation between the effect sizes (lnRR) and PC1. The correlation was estimated using a linear mixed-effects model with PC1 and ‘study’ as the fixed and random factors, respectively, and is significant at $p < 0.05$ based on two-sided F-tests with Satterthwaite approximation of degrees of freedom. R_m^2 and R_c^2 represent the marginal and conditional R^2 , which are the

proportion of variance explained by fixed effects and by both fixed and random effects, respectively. Black lines and gray shaded areas represent the mean and 95% confidence interval of the slope, respectively. PC1 depicting the leaf economics spectrum can be characterized by a single acquisitive-conservative axis. LA leaf area, leaf [C] leaf carbon concentration, leaf [N] leaf nitrogen concentration, leaf [P] leaf phosphorus concentration, SLA specific leaf area, leaf C:N leaf carbon/nitrogen ratio, LL leaf lifespan, leaf Pn leaf photosynthetic rate. Source data are provided as a Source Data file.

fixing legumes, which is crucial for overcoming their limited P acquisition capacity in low-P soils³³. Enhanced P availability supports symbiotic N_2 fixation and nodule formation, balancing the additional N from symbiotic N_2 fixation so that both N and P demands can be met^{15,34}. Deciduous plants displayed a stronger biomass response of plant biomass to P addition compared to evergreen plants (Fig. 3a). This may stem from their shorter leaf lifespan and faster photosynthetic rates during a short growing season, enabling efficient nutrient use^{14,16,35}. Conversely, C_4 plants exhibited a smaller biomass response to P addition than C_3 plants (Fig. 3a). This could be due to the evolutionary adaptation of C_4 species—many of which originated in tropical and subtropical regions—to thrive in P-poor soils, making them less responsive to ambient P enrichment^{16,36}. Additionally, C_4 plants often concentrate inorganic P in specialized cells dedicated to carbon fixation, potentially reducing their overall P requirements relative to C_3 plants^{36,37}. These distinct biomass responses to P addition among plant functional groups deepen our understanding of plant nutrient dynamics and are critical for improving predictive models of plant biomass accumulation and global carbon budgets in the context of increasing P deposition.

Despite these general trends, there was considerable variation in the responsiveness of plants to P addition across the globe. To understand the drivers of this variation, we explored how responses to P addition correlated with multiple leaf functional traits (Fig. 4). We discovered a positive association between the first principal component of leaf traits, which characterizes a single ‘conservative-acquisitive’ axis capturing most variation in the leaf economics spectrum^{20,22}, and the P addition-induced plant biomass response (Fig. 4). Traits associated with the acquisitive end of this axis, including high SLA, elevated leaf nitrogen concentration ([N]), high photosynthetic rates, and short leaf lifespan, typically indicate faster carbon assimilation and lower leaf construction costs. These traits are particularly advantageous for rapid plant growth, especially in seasonal climates with limited growing periods³⁸. Consequently, P addition may benefit acquisitive plants by facilitating their rapid growth potential.

Within the first principal component, SLA, leaf [N] and leaf C:N ratio emerged as the key functional traits, influencing the plant biomass responses. Specifically, stronger responses were observed in plants with higher SLA and leaf [N] and lower leaf C:N ratio (Fig. 5). SLA has been suggested as a reliable indicator for tracking variation in species’ responses to environmental changes³⁹. Plants with higher SLA typically exhibit faster photosynthetic rates, nutrient use efficiency, and growth rates, making them more responsive to P supply^{20,40}. In addition, high leaf [N] and low leaf C:N ratios indicate more efficient N uptake and a lower likelihood of N limitation in plants⁴¹, further amplifying the biomass response to P addition due to the functional coupling between these N and P⁴². We also found that the correlations between plant biomass response and key leaf functional traits were consistent across tropical, non-tropical, and global scale (Supplementary Fig. 11), suggesting the universal influence of leaf economic strategies on P-induced stimulation of terrestrial plant productivity. Furthermore, the importance of leaf economic strategies in driving the variation in plant biomass response to P addition has been consolidated by considering other potential influencing factors (Fig. 6, and Supplementary Figs. 6,7). Moreover, climate variables and soil properties exerted indirect effects on biomass responses through the first principal component of leaf traits (Fig. 6), likely reflecting interactions between climate and soil fertility in shaping global variation in leaf economic traits⁴³. Overall, these findings highlight the critical role of leaf functional traits in advancing our understanding of the mechanisms driving global variation in plant responses to P addition.

In addition to leaf functional traits, abiotic factors, such as climatic variables, soil properties and fertilization regimes, also influenced plant biomass responses to P addition (Supplementary Figs. 4,5). The influence of these abiotic factors primarily stems from their role in shaping the distribution and availability of P. Specially, biomass responses to P addition increased with rising MAT and MAP, likely due to the heightened P demand for plant growth and the reduced P availability caused by soil weathering, P leaching, and depletion of soil minerals in habitats like the humid tropical, subtropical, and dryland ecosystem^{8,44}. Consistent with this, we

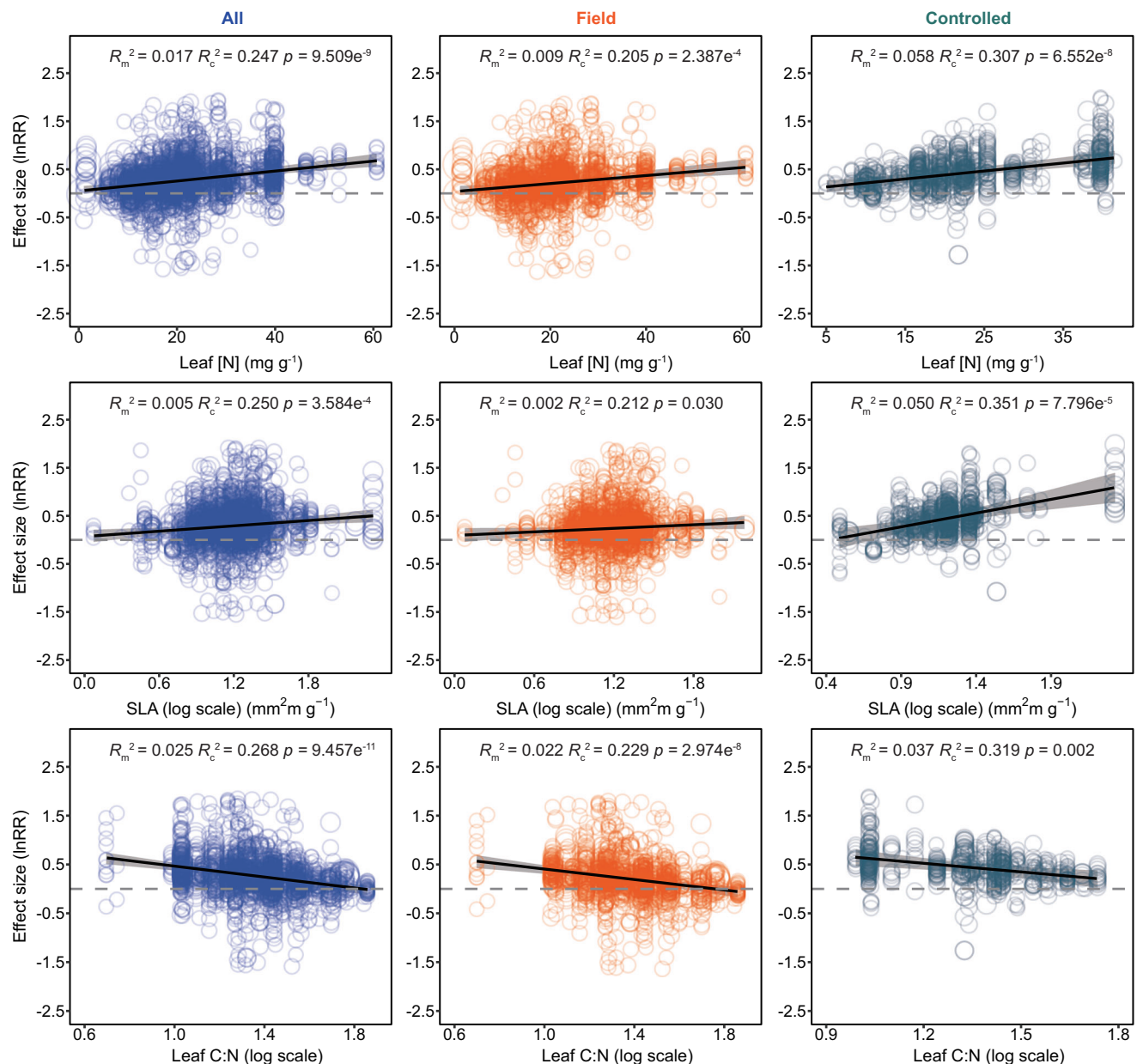


Fig. 5 | Correlations of the effect sizes of phosphorus (P) addition on plant biomass with functional traits across and within experimental settings. R_m^2 and R_c^2 represent the marginal and conditional R^2 , which are the proportion of variance explained by fixed effects and by both fixed and random effects, respectively. P values indicate statistical significance based on two-sided F -tests with Satterthwaite approximation of degrees of freedom in linear mixed models.

Black lines and gray shaded areas represent the mean and 95% confidence interval of the slope, respectively. Point sizes represent their corresponding weights. Moderator variables were log-transformed based on the corrected Akaike information criterion (AICc) from both linear and logarithmic mixed-effects models. leaf [N] leaf nitrogen concentration, SLA specific leaf area, leaf C:N leaf carbon/nitrogen ratio. Source data are provided as a Source Data file.

observed stronger biomass responses to P addition in tropical regions—where P limitation is widespread—and in other areas identified as P-limited based on high leaf N:P ratios (>20)⁴² (Supplementary Figs. 12,13). The negative correlation between the plant biomass response to P addition and soil total P concentration further supports this contention (Supplementary Fig. 5). Additionally, plant biomass responses were positively correlated with fertilization duration and P addition rates (Supplementary Fig. 4). This may be attributed to the cumulative increase in soil P availability from prolonged fertilization and higher P inputs, which can enhance plant growth and biomass accumulation⁴⁵. In turn, increased biomass production from sustained P enrichment may contribute to soil organic matter buildup⁴⁶. This accumulation can improve soil water-

holding capacity, cation-exchange capacity, and N retention⁴⁷, further promoting plant growth and biomass accumulation. Such positive feedback may amplify the effect of P addition, leading to continuous increases in plant biomass over time⁴⁸.

Our results regarding the effect of P addition on the biomass among different organs suggest that P addition shifts the functional equilibrium, favoring greater investment in aboveground organs. Specifically, P-fertilized plants showed higher mass fractions of leaves, stems and shoots, alongside lower root mass fractions and root-shoot ratios compared to non-fertilized plants (Fig. 7b). Given the essential role of P in photosynthesis⁴⁹ and the ubiquitous P limitation in global terrestrial plants⁷, P addition may enhance the carbon uptake capacity of photosynthetic organs, leading to increased leaf biomass^{49,50}. This supports

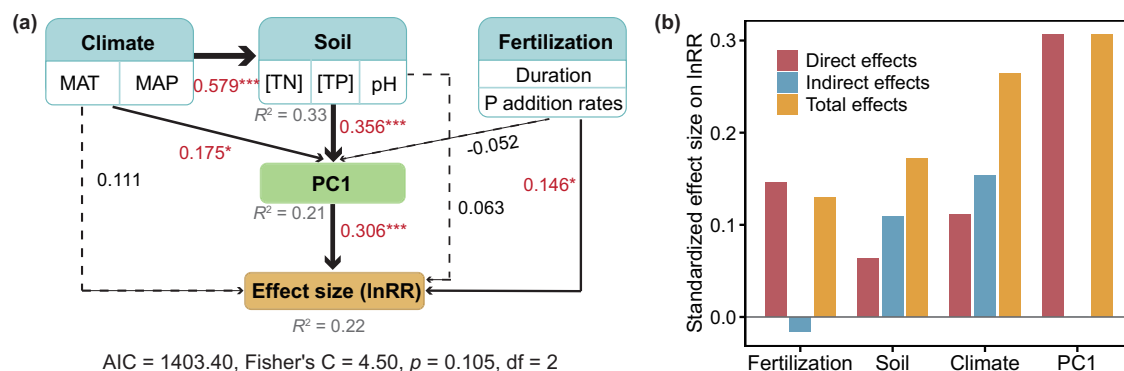


Fig. 6 | Piecewise structural equation modeling (piecewiseSEM) accounting for the direct and indirect effects of the parameters of the leaf economics spectrum and abiotic factors on the effect size of phosphorus (P) addition on plant biomass (lnRR). **a** The effects of PC1, climate, soil properties, and fertilization regimes on the effect size (lnRR) as revealed by piecewiseSEM. PC1 was derived from the principal component analysis (PCA) using the eight leaf functional traits as Fig. 4, and depicted the leaf economics spectrum, which can be characterized by a single acquisitive-conservative axis. Dark and blue arrows indicate positive and negative correlations, respectively. Solid and dashed lines indicate significant and insignificant correlations, respectively (* $p < 0.05$, ** $p < 0.01$, *** $p < 0.001$). Arrow width is proportional to the strength of the relationship. The numbers

adjacent to arrows are path coefficients, which indicate the standardized effect size of the relationship. The R^2 values beneath each response variable are the proportion of variance explained by both observed and latent variables. Global goodness-of-fit tests, including AIC, Fisher's C, and tests of directed separation ($p > 0.05$) are shown below the model. All statistical tests are conducted as two-sided.

b Standardized direct, indirect, and total effects derived from the piecewiseSEM. AIC Akaike information criterion, df degree of freedom, duration fertilization duration, soil [TN] soil total nitrogen concentration, soil [TP] soil total phosphorus concentration, MAT mean annual temperature, MAP mean annual precipitation. Source data are provided as a Source Data file.

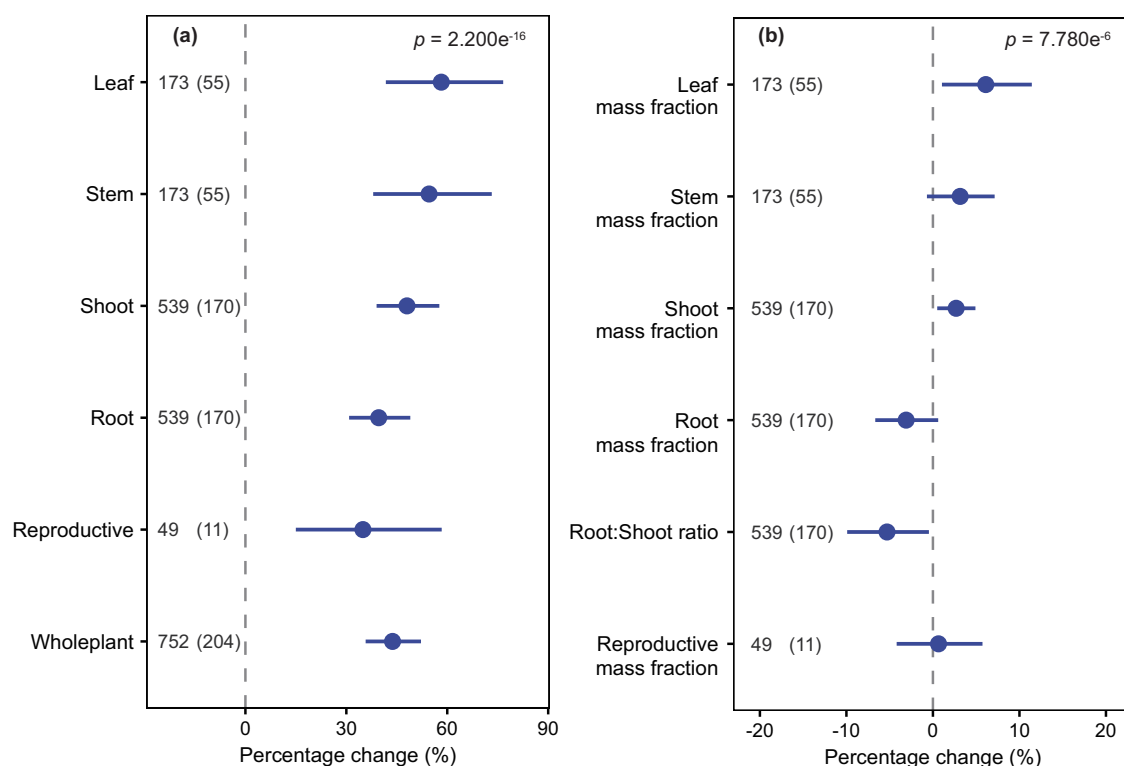


Fig. 7 | Organ-specific biomass responses to phosphorus (P) addition. **a** Average effects (%) of P addition on plant biomass among different plant organ types. **b** Average effects (%) of P addition on mass fractions and root-shoot ratio. Cross-comparisons among different plant organ types using the data with the total plant mass that are available for calculating the mass fractions and root-shoot ratio. Points and error bars represent the bootstrapped mean and 95% confidence interval, respectively. The numbers outside and inside parentheses indicate the number of observations and plant species, respectively. If the 95% confidence

interval does not overlap zero, the effects of P addition on plant biomass are considered significant (two-sided test, $p < 0.05$); otherwise, the effect of P addition is considered not significant. P values indicate statistical significance between organ types, based on linear mixed models with 'organ type' as a fixed factor and 'study' as random factor, tested using two-sided F-tests with Satterthwaite approximation of degrees of freedom. Source data are provided as a Source Data file.

the optimal partition theory, which posits that biomass allocation should maximize the acquisition of the most limiting growth resource⁵¹. In other words, plants will allocate more biomass belowground when the limiting resources are nutrients or water, and more biomass aboveground when the limiting factor is light^{30,52}. Overall, our findings suggest that increased allocation of biomass to aboveground organs under P addition may enhance the ability of plants to capture aboveground resources⁵³. Such biomass allocation patterns indicate that P addition might alter biomass accumulation strategies in global terrestrial plants, thereby influencing ecosystem carbon stocks in the future. Nonetheless, our results showed that the variation in P addition-induced response of plant biomass allocation was relatively stable across plant functional groups, and not strongly influenced by either leaf functional traits or abiotic factors (Supplementary Figs. 8–10). This finding suggests that plant biomass allocation compared with plant biomass was relatively conservative in response to P addition which is partly supported by a previous report of terrestrial plants in response to N addition³¹. We speculated that this finding arises from conserved P allocation strategies across functional groups, rooted in plants intrinsic operation as balanced systems under structural and functional constraints⁵⁴. Even P allocation among organs in *Artemisia* species appears comparatively insensitive to local environmental conditions⁵⁵. Thus, in response to P addition, P allocation among organs of plants across functional groups may remain conservative, thereby maintaining the conservatism of biomass allocation across functional groups. Furthermore, leaf economic strategies may be poor proxies for whole-plant adaptation strategies reflected by biomass allocation⁵⁶.

With these findings, our work has important implications for estimating carbon stocks and predicting future vegetation dynamics under enhanced anthropogenic P deposition. While most previous meta-analyses have focused on the effect of environmental factors and experimental settings on plant biomass responses to P addition^{7,8,57}, our study highlights the functional type-specific and trait-mediated responses of terrestrial plants to P addition. In particular, our findings emphasize the contrasting adaptive strategies of plants, which are governed by the leaf economics spectrum, representing a continuum from acquisitive to conservative trait syndromes^{20,22}. Understanding these adaptive growth strategies is key for predicting changes in plant community structure, vegetation dynamics, and ecosystem functioning under future scenarios of enhanced P deposition. Furthermore, our findings provide empirical evidence that can inform the development of terrestrial biosphere and carbon budget models incorporating P-cycling processes⁵⁸. The variation across plant functional groups, trait-based effects, and contrasting biomass-allocation strategies are key mechanisms for the acclimation of terrestrial plants to P addition, and their implementation into terrestrial biosphere models⁵⁹, may enhance predictions of future biogeochemical cycles and carbon dynamics⁶⁰. Overall, our global-scale findings contribute to a better understanding of the capacity of terrestrial plants to increase productivity in response to rising P deposition, which is critical for forecasting the future global land carbon sink.

Methods

Data collection

We systematically searched for peer-reviewed publications related to the effect of P addition on plant biomass and its allocation using the Web of Science and China National Knowledge Infrastructure until 9 October 2023. The searching terms and their combinations are listed in Supplementary Table 1. Additionally, we screened five previous meta-analyses^{7,8,57,61,62} to complete our literature database.

To minimize selection bias and increase data comparability, we selected publications that met the following criteria: (i) P addition experiments were conducted in controlled environments (e.g., greenhouse, growth chamber) or field environments, and must include

at least one of the following variables: biomass of the whole plant, leaves, stems, roots, shoots or reproductive organs; (ii) both the control and P addition treatments groups were under the same experimental settings, and only the control and P addition treatments were selected in case P addition treatment was additionally combined with other treatments (e.g., factorial experiments); (iii) treatment with P fertilizers containing N, such as diammonium phosphate, were excluded; (iv) the biomass response of single species was reported in both control and P addition treatments, but crops and transgenic plants were excluded; and (v) the mean and sample size for both control and P addition treatments could be directly extracted or calculated for each study. The selection process is illustrated in a PRISMA flow diagram (Supplementary Fig. 1).

For each selected publication, the means and sample sizes were extracted from tables or text. When results were reported in figures, data were extracted using WebPlotDigitizer (version 4.6, <https://automeris.io/wpd/>). After extraction and compilation, 3,514 observations and 423 species from 317 publications (86 controlled and 234 field environments) were included in our database. Based on this database, we also calculated the fraction of total plant biomass allocating to different organs, and a total of 5548 observations were finally included in this meta-analysis. Environmental variables, such as MAT, MAP, location coordinate (latitude and longitude), fertilization regimes (duration, P addition rates, and P addition forms) and experimental settings (controlled or field) were also extracted from the publications. If MAP and MAT data were not directly reported, they were derived from the WorldClim database (<http://www.worldclim.org/>) based on the experiment's geolocation. Additionally, background soil properties for the experiments (concentrations of soil total P (g kg^{-1}) and available P (mg kg^{-1}), soil total N (g kg^{-1}) and soil pH) were extracted from the publications. The available P concentrations was not extracted due to the lack of a unified measurement method in the publications. For field experiments lacking records of soil properties in the original publications, these data were extracted from the GSDE (Global Soil Dataset for Earth System Model) datasets.

For each species, the scientific names were first verified using The Plant List (<http://www.theplantlist.org>). Plant functional groups were then identified according to previous publications^{63,64}, as well as online databases, including the TRY plant trait database (<http://www.try-db.org>)³¹, the Flora of China (<http://frps.eflora.cn/>), and Wikipedia (<https://en.wikipedia.org/wiki>). Each species was categorized into different growth forms (tree, shrub, forb and graminoid), mycorrhizal types (arbuscular mycorrhizal (AM) or ectomycorrhizal (EcM)), photosynthetic pathways (C_3 or C_4), and plant N_2 fixing taxa (N_2 -fixing or non- N_2 -fixing species). Woody species were further classified into evergreen or deciduous and coniferous or broadleaved species, while non-woody species were categorized into annual or perennial plants. Additionally, leaf functional traits, including leaf area (LA, mm^2), leaf carbon concentration ([C], mg g^{-1}), leaf [N] (mg g^{-1}), leaf [P] (mg g^{-1}), SLA ($\text{mm}^2 \text{mg}^{-1}$), leaf C:N ratio, leaf N:P ratio, leaf photosynthetic rate (Pn , $\mu\text{mol g}^{-2} \text{s}^{-1}$), and leaf lifespan (LL) for each species were collected from the control data in the publications. If trait data were not reported, they were derived from the TRY plant trait database¹⁹. The leaf N:P ratio was mainly used to classify the nutrient limitation types of the studied plants based on leaf N:P thresholds of 10 and 20⁴². And the average effect of P addition on plant biomass was 26% (95% confidence interval (CI): 19.8–35.9%) under N limitation (leaf N:P < 10) and 38% (25.4–51.2%) under P limitation (leaf N:P > 20, Supplementary Fig. 13), suggesting that plants under P limitation showed a significantly greater response of the biomass to P addition than those under N limitation.

Data analysis

We used the logarithmic response ratio (lnRR) as measure of effect size to quantify the effect of P addition on plant biomass and its allocation⁶¹.

The lnRR and weight (W_r) for each observation were calculated as:

$$\ln \text{RR} = \ln(\bar{X}_t / \bar{X}_c) = \ln \bar{X}_t - \ln \bar{X}_c \quad (1)$$

$$W_r = (N_c \times N_t) / (N_c + N_t) \quad (2)$$

where \bar{X}_c and \bar{X}_t are the means of the observed values for control and P addition treatments, respectively. W_r is the weight for each observation, and N_c and N_t are the sample sizes in the control and P addition treatments, respectively. Sample sizes were used to calculate the weight because sampling variances were missing in 124 of the 317 publications. This method for determining weight has been widely used in previous meta-analyses^{61,65}. To evaluate the robustness of our results, we subsequently conducted statistical tests for publication bias using Egger's test⁶⁶. Results indicated that there was no significant publication bias for each variable (Supplementary Table 2).

To characterize the phylogenetic structure of lnRR, we first generated phylogenetic trees of the 423 species with the 'V.PhyloMaker' package based on a mega-tree of vascular plants⁶⁷ and then estimated phylogenetic signal using Pagel's λ in the 'Geiger' package⁶⁸. Pagel's λ is a scaling parameter between 0 and 1, where $\lambda = 1$ indicates a perfect phylogenetic signal, while $\lambda = 0$ indicates no phylogenetic signal, aligning with trait evolution under Brownian motion⁶⁹. And $p < 0.05$ indicates a significant phylogenetic signal. Pagel's λ was selected for its ability to distinguish complex trait evolution models, reliably measure effect size, and its suitability for large phylogenies with over 50 species⁷⁰. Second, we compared the variability in lnRR across five phylogenetic groups, namely pteridophytes, gymnosperms, magnoliids, monocots, and eudicots ordered by evolutionary age from oldest to youngest⁴¹.

To estimate the average P-addition effect across or within different functional groups and organ types, we then constructed linear mixed-effects models with 'study' and ' W_r ' as the random factor and weight respectively, fitting with restricted maximum likelihood using the 'lmer' function in the 'lme4' package⁶¹.

$$\ln \text{RR} = \beta_0 + \pi_{\text{study}} + \varepsilon \quad (3)$$

where β_0 represents the intercepts, π_{study} denotes the random effects to account for autocorrelation among observations within each study and ε represents the sampling error. We checked the normality of the model residuals using the 'check_normality' function in the 'performance' package. When the normality assumption was violated, a new 95% confidence interval (CI) was generated by using a bootstrapping method with 999 iterations in the 'boot' package. For a better interpretation, we converted the lnRR and its associated 95% CI to percentage change as follows:

$$\text{Percentage change (\%)} = (e^{\ln \text{RR}} - 1) \times 100\% \quad (4)$$

To quantify the influence of leaf functional traits on P-addition effect on plant biomass and its allocation, we first performed a principal component analysis (PCA) to illustrate the multivariate associations of leaf functional traits²⁰. The first principal component (PC1), representing the acquisitive versus conservative axis of the leaf economics spectrum, explained 40.1% of the total variation of these traits (Fig. 4). Then, the PC1 was used to examine how plant biomass responses to P addition correlate with leaf economic strategies. To analyze this correlation, we used linear mixed-effects models to assess the link between lnRR and PC1.

Furthermore, we identified the key leaf functional traits that contributed to PC1 and explored the correlations between lnRR and each of those key traits using the linear mixed-effects model. Meanwhile, to clarify the effects of other potential influencing factors on

lnRR, we also explored the correlations of lnRR with climate variables, soil properties, and fertilization regimes. The correlations between lnRR and P addition forms exhibited insignificant differences across and within experimental settings, and thus P addition forms was excluded from subsequent analysis. Whether moderator variables were log-transformed was based on the corrected Akaike information criterion (AICc) derived from both linear and logarithmic mixed-effects models. Here, moderator variables were treated as fixed factors, and 'study' was included as random factor. The marginal and conditional R^2 were computed using the 'r.squaredGLMM' function in the 'MuMIn' package⁷¹. Finally, the model results were visually illustrated using the 'visreg' function within the 'visreg' package.

In addition, we quantified the relative importance of leaf functional traits and abiotic factors (climate variables, soil properties, and fertilization regimes) on lnRR variabilities through the boosted regression tree (BRT) analyses. The moderator variables used in this analysis were pre-screened based on variance inflation factors ($VIF < 5$) to avoid multicollinearity. All moderator variables were scaled before modeling. Here, leaf functional traits were considered through two ways in the BRT analyses, with one way using the PC1 of leaf functional traits and another using the key functional traits associated with PC1. The BRT analyses were conducted using the 'gbm' package⁷. Specific parameter settings were based on a previous study⁷, including a Gaussian error distribution, tree complexity of 2, a learning rate of 0.005, 10 fold cross-validation and a bag fraction of 0.75. Model performance was evaluated using cross-validation correlation (CV). The relative importance of each predictor derived from the BRT was represented as the percentage of the total variation explained by the models. Finally, partial dependence plots of BRT analysis were generated to visually illustrate the effects of each predictor.

To evaluate the direct and indirect effects of leaf functional traits (indicated by PC1), climate variables, soil properties, and fertilization regimes on lnRR, we conducted a structural equation modeling (SEM) analysis using 'piecewiseSEM' and 'lme4' packages⁷². The SEM analysis enables the analysis of complex causal networks and the testing of hypotheses regarding cause-effect relationships based on a priori information. In our study, a key underlying assumption in the a priori SEM model is that abiotic factors can indirectly influence the variation in lnRR through their effects on leaf functional traits. All the moderator variables included in this model were first divided into 'composite variables' and then included in the SEM. The factors of climate, soil, and fertilization regimes in the SEM were the same as those used in the BRT analyses. A good fit of the SEM was evaluated using Fisher's C value, which was non-significant ($p > 0.05$). All statistical analyses were conducted using R software version 4.3.3⁷³.

Reporting summary

Further information on research design is available in the Nature Portfolio Reporting Summary linked to this article.

Data availability

The data generated in this study, including raw data and source data underlying the figures and tables, have been deposited in Figshare at <https://doi.org/10.6084/m9.figshare.29154539>. Mean annual temperature and mean annual precipitation at each site were extracted from the WorldClim database (<http://www.worldclim.org/>). Soil characteristics including soil pH, soil total P and soil total N concentrations were extracted from GSDE (Global Soil Dataset for Earth System Model) datasets. Leaf functional traits were extracted from the TRY plant trait database (<http://www.try-db.org>). Source data are provided with this paper.

Code availability

The code generated in this study have been deposited in Figshare at <https://doi.org/10.6084/m9.figshare.29154539>.

References

- Walker, W. S. et al. The global potential for increased storage of carbon on land. *Proc. Natl Acad. Sci. USA* **119**, e2111312119 (2022).
- Dolezal, J., Jandova, V., Macek, M. & Liancourt, P. Contrasting biomass allocation responses across ontogeny and stress gradients reveal plant adaptations to drought and cold. *Funct. Ecol.* **35**, 32–42 (2021).
- Zhou, L. Y. et al. Global systematic review with meta-analysis shows that warming effects on terrestrial plant biomass allocation are influenced by precipitation and mycorrhizal association. *Nat. Commun.* **13**, 4914 (2022).
- Lambers, H. Phosphorus acquisition and utilization in plants. *Annu. Rev. Plant Biol.* **73**, 17–42 (2022).
- Peñuelas, J. et al. Human-induced nitrogen-phosphorus imbalances alter natural and managed ecosystems across the globe. *Nat. Commun.* **4**, 2934 (2013).
- Pan, Y. P. et al. Enhanced atmospheric phosphorus deposition in asia and europe in the past two decades. *Atmos. Ocean. Sci. Lett.* **14**, 100051 (2021).
- Hou, E. Q. et al. Global meta-analysis shows pervasive phosphorus limitation of aboveground plant production in natural terrestrial ecosystems. *Nat. Commun.* **11**, 637 (2020).
- Hou, E. Q. et al. Latitudinal patterns of terrestrial phosphorus limitation over the globe. *Ecol. Lett.* **24**, 1420–1431 (2021).
- Woś, B. et al. Nutrient uptake efficiency and stoichiometry for different plant functional groups on spoil heap after hard coal mining in upper silesia, poland. *Sci. Total Environ.* **924**, 171612 (2024).
- Gao, X. L., Li, X. G., Zhao, L. & Kuzyakov, Y. Regulation of soil phosphorus cycling in grasslands by shrubs. *Soil Biol. Biochem.* **133**, 1–11 (2019).
- Yan, L., Tang, D., Pang, J. Y. & Lambers, H. Root carboxylate release is common in phosphorus-limited forest ecosystems in China: using leaf manganese concentration as a proxy. *Plant Soil* 1–16 <https://doi.org/10.1007/s11104-024-06791-8> (2024).
- Prieto, I. & Querejeta, J. I. Simulated climate change decreases nutrient resorption from senescing leaves. *Glob. Change Biol.* **26**, 1795–1807 (2020).
- Chen, X. P. et al. Divergent leaf nutrient-use strategies of coexistent evergreen and deciduous trees in a subtropical forest. *J. Plant Ecol.* **16**, rtac093 (2023).
- Sophia, G., Caldararu, S., Stocker, B. & Zaehle, S. Leaf habit and nutrient availability drive leaf nutrient resorption globally. *EGU-sphere* **687**, 1–39 (2024).
- Toro, L. et al. Phosphorus limitation of early growth differs between nitrogen-fixing and nonfixing dry tropical forest tree species. *N. Phytol.* **237**, 766–779 (2023).
- Huang, X. Z. et al. Global distributions of foliar nitrogen and phosphorus resorption in forest ecosystems. *Sci. Total Environ.* **871**, 162075 (2023).
- Bustamante, M. M. et al. Effects of nutrient additions on plant biomass and diversity of the herbaceous-subshrub layer of a Brazilian savanna (Cerrado). *Plant Ecol.* **213**, 795–808 (2012).
- Liu, C. C. et al. Effects of nitrogen, phosphorus and potassium addition on the productivity of a karst grassland: Plant functional group and community perspectives. *Ecol. Eng.* **117**, 84–95 (2018).
- Kattge, J. et al. TRY plant trait database-enhanced coverage and open access. *Glob. Change Biol.* **26**, 119–188 (2020).
- Wright, I. J. et al. The worldwide leaf economics spectrum. *Nature* **428**, 821–827 (2004).
- Chollet, S. et al. Combined effects of climate, resource availability, and plant traits on biomass produced in a mediterranean rangeland. *Ecology* **95**, 737–748 (2014).
- Reich, P. B. The world-wide ‘fast-slow’ plant economics spectrum: a traits manifesto. *J. Ecol.* **102**, 275–301 (2014).
- Prado-Junior, J. A. et al. Conservative species drive biomass productivity in tropical dry forests. *J. Ecol.* **104**, 817–827 (2016).
- Poorter, L. & Bongers, F. Leaf traits are good predictors of plant performance across 53 rain forest species. *Ecology* **87**, 1733–1743 (2006).
- Guo, X. H. et al. Response of plant functional traits to nitrogen enrichment under climate change: A meta-analysis. *Sci. Total Environ.* **834**, 155379 (2022).
- Puglielli, G., Laanisto, L., Poorter, H. & Niinemets, Ü Global patterns of biomass allocation in woody species with different tolerances of shade and drought: evidence for multiple strategies. *N. Phytol.* **229**, 308–322 (2021).
- Brouwer, R. Some aspects of the equilibrium between overground and underground plant parts. *Jaarb. van. het Inst. voor Biologisch en. Scheikundig Onderz. aan Landbouwgewassen* **213**, 31–39 (1963).
- Ma, H. Z. et al. The global distribution and environmental drivers of aboveground versus belowground plant biomass. *Nat. Ecol. Evol.* **5**, 1110–1122 (2021).
- Müller, I., Schmid, B. & Weiner, J. The effect of nutrient availability on biomass allocation patterns in 27 species of herbaceous plants. *Perspect. Plant Ecol. Evol. Syst.* **3**, 115–127 (2000).
- Yue, K. et al. Nitrogen addition affects plant biomass allocation but not allometric relationships among different organs across the globe. *J. Plant Ecol.* **14**, 361–371 (2021).
- Feng, H. L. et al. Nitrogen addition promotes terrestrial plants to allocate more biomass to aboveground organs: A global meta-analysis. *Glob. Change Biol.* **29**, 3970–3989 (2023).
- McCarthy, M. C. & Enquist, B. J. Consistency between an allometric approach and optimal partitioning theory in global patterns of plant biomass allocation. *Funct. Ecol.* **21**, 713–720 (2007).
- Pang, J. Y., Ryan, M. H., Lambers, H. & Siddique, K. H. Phosphorus acquisition and utilisation in crop legumes under global change. *Curr. Opin. Plant Biol.* **45**, 248–254 (2018).
- Augusto, L., Delerue, F., Gallet-Budynek, A. & Achat, D. L. Global assessment of limitation to symbiotic nitrogen fixation by phosphorus availability in terrestrial ecosystems using a meta-analysis approach. *Glob. Biogeochem. Cycles* **27**, 804–815 (2013).
- Krishna, M. & Garkoti, S. C. Evergreen and deciduous tree species show distinct strategies to synchronize with seasonality in mid-elevational forests of central himalaya. *Ecol. Manag.* **526**, 120567 (2022).
- Halsted, M. & Lynch, J. Phosphorus responses of C₃ and C₄ species. *J. Exp. Bot.* **47**, 497–505 (1996).
- Ghannoum, O. et al. The sensitivity of photosynthesis to phosphorus deficiency differs between C₃ and C₄ tropical grasses. *Funct. Plant Biol.* **35**, 213–221 (2008).
- Castorena, M., Olson, M. E., Enquist, B. J. & Fajardo, A. Toward a general theory of plant carbon economics. *Trends Ecol. Evol.* **37**, 829–837 (2022).
- Kandlikar, G. S., Kleinhesselink, A. R. & Kraft, N. J. Functional traits predict species responses to environmental variation in a california grassland annual plant community. *J. Ecol.* **110**, 833–844 (2022).
- Avalos, G. Specific leaf area (SLA) serves as a proxy to predict total carbon content in understory individuals of the neotropical canopy palm *Socratea exorrhiza*. *Trees* **37**, 1831–1840 (2023).
- Zhang, J. H. et al. Variation and evolution of C:N ratio among different organs enable plants to adapt to N-limited environments. *Glob. Change Biol.* **26**, 2534–2543 (2020).
- Güsewell, S. N:P ratios in terrestrial plants: variation and functional significance. *N. Phytol.* **164**, 243–266 (2004).
- Joswig, J. S. et al. Climatic and soil factors explain the two-dimensional spectrum of global plant trait variation. *Nat. Ecol. Evol.* **6**, 36–50 (2022).
- Cunha, H. F. V. et al. Direct evidence for phosphorus limitation on amazon forest productivity. *Nature* **608**, 558–562 (2022).

45. Sun, Y. & Chen, X. L. Phosphorus fertilization enhances terrestrial carbon cycling in phosphorus-deficient ecosystems. *J. Environ. Manag.* **351**, 119941 (2024).
46. Luo, X. Z., Zhang, L. L., Lin, Y. B., Wen, D. Z. & Hou, E. Q. Nitrogen availability mediates soil organic carbon cycling in response to phosphorus supply: a global meta-analysis. *Soil Biol. Biochem.* **185**, 109158 (2023).
47. Hobbie, S. E. Plant species effects on nutrient cycling: revisiting litter feedbacks. *Trends Ecol. Evol.* **30**, 357–363 (2015).
48. Seabloom, E. W. et al. Increasing effects of chronic nutrient enrichment on plant diversity loss and ecosystem productivity over time. *Ecology* **102**, e03218 (2021).
49. Ellsworth, D. S. et al. Convergence in phosphorus constraints to photosynthesis in forests around the world. *Nat. Commun.* **13**, 5005 (2022).
50. Wright, S. J. Low phosphorus levels limit carbon capture by amazonian forests. *Nature* **608**, 476–477 (2022).
51. Poorter, H. et al. Biomass allocation to leaves, stems and roots: Meta-analyses of interspecific variation and environmental control. *N. Phytol.* **193**, 30–50 (2012).
52. Li, C. B. et al. Precipitation and nitrogen addition enhance biomass allocation to aboveground in an alpine steppe. *Ecol. Evol.* **9**, 12193–12201 (2019).
53. Poorter, H. & Nagel, O. The role of biomass allocation in the growth response of plants to different levels of light, CO₂, nutrients and water: A quantitative review. *Aust. J. Plant Physiol.* **27**, 595–607 (2000).
54. Zhao, N. et al. Conservative allocation strategy of multiple nutrients among major plant organs: from species to community. *J. Ecol.* **108**, 267–278 (2020).
55. Gong, H. et al. Conservative allocation strategy of nitrogen and phosphorus among leaves, stems and roots of *Artemisia* species. *BMC Plant Biol.* **25**, 1–11 (2025).
56. Mason, C. M., Goolsby, E. W., Davis, K. E., Bullock, D. V. & Donovan, L. A. Importance of whole-plant biomass allocation and reproductive timing to habitat differentiation across the North American sunflowers. *Ann. Bot.* **119**, 1131–1142 (2017).
57. Li, Y., Niu, S. L. & Yu, G. R. Aggravated phosphorus limitation on biomass production under increasing nitrogen loading: a meta-analysis. *Glob. Change Biol.* **22**, 934–943 (2016).
58. Jiang, M. K. et al. Carbon-phosphorus cycle models overestimate CO₂ enrichment response in a mature *Eucalyptus* forest. *Sci. Adv.* **10**, ead15822 (2024).
59. Thum, T. et al. A new model of the coupled carbon, nitrogen, and phosphorus cycles in the terrestrial biosphere (QUINCY v1.0; revision 1996). *Geosci. Model Dev.* **12**, 4781–4802 (2019).
60. Wieder, W. R., Cleveland, C. C., Smith, W. K. & Todd-Brown, K. Future productivity and carbon storage limited by terrestrial nutrient availability. *Nat. Geosci.* **8**, 441–444 (2015).
61. Feng, J. G., Song, Y. J. & Zhu, B. Ecosystem-dependent responses of soil carbon storage to phosphorus enrichment. *N. Phytol.* **238**, 2363–2374 (2023).
62. Jiang, J. et al. Interactive effects of nitrogen and phosphorus additions on plant growth vary with ecosystem type. *Plant Soil* **440**, 523–537 (2019).
63. Tedersoo, L. et al. Global database of plants with root-symbiotic nitrogen fixation: NodDB. *J. Veg. Sci.* **29**, 560–568 (2018).
64. Soudzilovskaia, N. A. et al. FungalRoot: global online database of plant mycorrhizal associations. *N. Phytol.* **227**, 955–966 (2020).
65. Gurevitch, J., Koricheva, J., Nakagawa, S. & Stewart, G. Meta-analysis and the science of research synthesis. *Nature* **555**, 175–182 (2018).
66. Egger, M., Smith, G. D., Schneider, M. & Minder, C. Bias in meta-analysis detected by a simple, graphical test. *Br. Med. J.* **315**, 629–634 (1997).
67. Jin, Y. & Qian, H. V. PhyloMaker: An R package that can generate very large phylogenies for vascular plants. *Ecography* **42**, 1353–1359 (2019).
68. Harmon, L. J., Weir, J. T., Brock, C. D., Glor, R. E. & Challenger, W. Geiger: investigating evolutionary radiations. *Bioinformatics* **24**, 129–131 (2008).
69. Pagel, M. Inferring the historical patterns of biological evolution. *Nature* **401**, 877–884 (1999).
70. Münkemüller, T. et al. How to measure and test phylogenetic signal. *Methods Ecol. Evol.* **3**, 743–756 (2012).
71. Bartoň, K. *MuMIn: multi-model inference*. R package version 1.46.0. <https://CRAN.R-project.org/package=MuMIn> (2022).
72. Zhang, J. K., Yu, W. Y., Wang, Y., Huang, Z. & Liu, G. F. Effects of climate, soil, and leaf traits on nutrient resorption efficiency and proficiency of different plant functional types across arid and semi-arid regions of northwest China. *BMC Plant Biol.* **24**, 1093 (2024).
73. R Core Team. *R: a language and environment for statistical computing*, v.4.3.3. (R Foundation for Statistical Computing, Vienna, Austria, 2024).

Acknowledgements

This work was supported by supported by National Natural Science Foundation of China (nos. 32471573, 32401379, 31988102), and Key Talent Project of the State Key Laboratory of Vegetation and Environmental Change (LVEC-2023rc01). C.M.Z. was funded by the SNSF Ambizione grant PZ00P3_193646. Josep Peñuelas and Jordi Sardans were supported by the Spanish Government grants PID2020115770RB-I, PID2022-140808NB-I00, and TED2021-132627 B-I00 funded by MCIN, AEI/10.13039/501100011033 European Union Next Generation EU/PRTR, and the Fundación Ramón Areces grant CIVP20A6621. Funding was provided to HL by the Deputy Vice Chancellor (Research) at the University of Western Australia. J. Wu was supported by the National Natural Science Foundation of China (#31922090) and the Innovation and Technology Fund (Funding Support to State Key Laboratory of Agrobiotechnology).

Author contributions

Z.Y. and N.Y. designed the study. N.Y. collected the data. N.Y. and Z.Y. analyzed the data with inputs from J.G.F. N.Y. wrote the first draft of the manuscript with constructive input from Z.Y. C.Z., T.C., J.G.F., J.W., X.C., W.H., B.S., D.H., L.A., K.Y., E.H., M.J., H.F., Z.C., W.W., A.X., C.C., J.S., Y.L., J.P., H.L. and J.Y.F. contributed significantly to the writing and revising of the manuscript. Then N.Y. and Z.Y. revised the successive following versions of the manuscript with assistance from all of the authors, particularly J.Y.F., J.G.F., C.Z., H.L., J.S. and J.P.

Competing interests

The authors declare no competing interests.

Additional information

Supplementary information The online version contains supplementary material available at <https://doi.org/10.1038/s41467-025-60633-4>.

Correspondence and requests for materials should be addressed to Zhengbing Yan.

Peer review information *Nature Communications* thanks Oskar Franklin and the other, anonymous, reviewer(s) for their contribution to the peer review of this work. A peer review file is available.

Reprints and permissions information is available at <http://www.nature.com/reprints>

Publisher's note Springer Nature remains neutral with regard to jurisdictional claims in published maps and institutional affiliations.

Open Access This article is licensed under a Creative Commons Attribution-NonCommercial-NoDerivatives 4.0 International License, which permits any non-commercial use, sharing, distribution and reproduction in any medium or format, as long as you give appropriate credit to the original author(s) and the source, provide a link to the Creative Commons licence, and indicate if you modified the licensed material. You do not have permission under this licence to share adapted material derived from this article or parts of it. The images or other third party material in this article are included in the article's Creative Commons licence, unless indicated otherwise in a credit line to the material. If material is not included in the article's Creative Commons licence and your intended use is not permitted by statutory regulation or exceeds the permitted use, you will need to obtain permission directly from the copyright holder. To view a copy of this licence, visit <http://creativecommons.org/licenses/by-nc-nd/4.0/>.

© The Author(s) 2025

¹State Key Laboratory of Forage Breeding-by-Design and Utilization; Key Laboratory of Vegetation and Environmental Change, Institute of Botany, Chinese Academy of Sciences, Xiangshan, Beijing, China. ²China National Botanical Garden, Beijing, China. ³University of Chinese Academy of Sciences, Yuquanlu, Beijing, China. ⁴Institute of Integrative Biology, ETH Zurich (Swiss Federal Institute of Technology), Universitätsstrasse 16, Zurich, Switzerland. ⁵Ministry of Education Key Laboratory for Ecology and Resource Use of the Mongolian Plateau, Inner Mongolia Key Laboratory for Grassland Ecology, and School of Ecology and Environment, Inner Mongolia University, Huhhot, China. ⁶National Key Laboratory of Water Disaster Prevention, Jiangsu Key Laboratory of Soil and Water Processes in Watershed, College of Geography and Remote Sensing, Hohai University, Nanjing, China. ⁷School of Biological Sciences, The University of Hong Kong, Hong Kong, China. ⁸Institute for Climate and Carbon Neutrality, The University of Hong Kong, Hong Kong, China. ⁹State Key Laboratory of Agrobiotechnology, Chinese University of Hong Kong, Hong Kong, China. ¹⁰State Key Laboratory of Subtropical Silviculture, Zhejiang A&F University, Hangzhou, China. ¹¹Key Laboratory of Plant-Soil Interactions, Ministry of Education, College of Resources and Environmental Sciences, China Agricultural University, Beijing, China. ¹²Institute of Geography, University of Bern, Bern, Switzerland. ¹³Department of Biological Sciences, Tennessee State University, Nashville, TN, USA. ¹⁴INRAE, Bordeaux Sciences Agro, ISPA, Villenave d'Ornon, France. ¹⁵Key Laboratory for Humid Subtropical Eco-Geographical Processes of the Ministry of Education, School of Geographical Sciences, Fujian Normal University, Fuzhou, Fujian, China. ¹⁶Guangdong Provincial Key Laboratory of Applied Botany and Key Laboratory of Vegetation Restoration and Management of Degraded Ecosystems, South China Botanical Garden, Chinese Academy of Sciences, Guangzhou, China. ¹⁷Key Laboratory of National Forestry and Grassland Administration on Plant Conservation and Utilization in Southern China, Guangzhou, China. ¹⁸College of Life Sciences, Zhejiang University, Hangzhou, China. ¹⁹Key Laboratory of Ministry of Education for Genetics and Germplasm Innovation of Tropical Special Trees and Ornamental Plants, School of Tropical Agriculture and Forestry (School of Agricultural and Rural Affairs, School of Rural Revitalization), Hainan University, Haikou, Hainan 570228, China. ²⁰Australian Rivers Institute, Griffith University, Nathan, QLD, Australia. ²¹School of Environment and Science, Griffith University, Nathan, QLD, Australia. ²²CSIC, Global Ecology Unit, CREAM-CSIC-UAB, Bellaterra, Barcelona, Catalonia, Spain. ²³CREAF, Cerdanyola del Vallès, Barcelona, Catalonia, Spain. ²⁴Soil and Crop Sciences Section, School of Integrative Plant Science, Cornell University, Ithaca, New York, USA. ²⁵School of Biological Sciences, The University of Western Australia, 35 Stirling Highway, Perth, WA, Australia. ²⁶Institute of Ecology, College of Urban and Environmental Sciences, Peking University, Beijing, China. ²⁷Key Laboratory for Earth Surface Processes of the Ministry of Education, Peking University, Beijing, China. ✉e-mail: zbyan@ibcas.ac.cn